Alexandria Engineering Journal (2022) 61, 4359–4369

HOSTED BY

Alexandria University

Alexandria Engineering Journal

www.elsevier.com/locate/aej
www.sciencedirect.com

Exergy analysis of two indirect evaporative cooling experimental prototypes

Ana M. Blanco-Marigorta [a,*], Ana Tejero-González [b], Javier M. Rey-Hernández [c], Eloy Velasco Gómez [b], Richard Gaggioli [d]

[a] Universidad de Las Palmas de Gran Canaria, Las Palmas, GC, Spain
[b] Universidad de Valladolid, Valladolid, Spain
[c] Universidad Europea Miguel de Cervantes, Valladolid, Spain
[d] Marquette University, Milwaukee, WI, USA

Received 20 July 2021; revised 14 September 2021; accepted 27 September 2021
Available online 09 October 2021

KEYWORD

Indirect evaporative cooling;
Heat recovery;
Plastic heat exchanger;
Exergy analysis;
Exergetic efficiency

Abstract This paper deals with the exergy analysis of two experimental prototypes consisting of indirect evaporative cooling systems with different constructive characteristics. Both prototypes have been designed and manufactured in the Thermal Engineering Laboratory of the University of Valladolid. They are made of polycarbonate hollow panels of different cross section and connected into a heat recovery cycle. Each prototype has been tested at 4 levels of outdoor air volume flow (from 125 to 400 $m^3 \cdot h^{-1}$) and 4 levels of dry bulb temperature (from 25 to 40 °C). For each of the 16 different operating conditions the exergy destructed by each prototype has been calculated. Results show that the higher the dry bulb temperature at the primary air inlet, the higher the exergy destruction and the exergy losses. The exergy destruction increases when the wet bulb depression temperature of the secondary air inlet decreases, leading to more inefficient configurations. The value of the exergetic efficiency is in the order of 2–12 %. The optimum combination of operating conditions at any inlet temperature of the primary air can be proposed as: 300 $m^3 h^{-1}$ and 200 $m^3 h^{-1}$. for the wide and narrow plates prototype, respectively.

1. Introduction

It is usually considered that aprox. 20%−40% of the European final energy consumption is associated with the building sector. Within this sector, the main energy consumption – around 68%– is due to thermal conditioning. Therefore, it is not surprising that, in Europe, the building sector is considered as the one with highest energy saving potential. In Spain, the

* Corresponding author.
E-mail addresses: anamaria.blanco@ulpgc.es (A.M. Blanco-Marigorta), anatej@eii.uva.es (A. Tejero-González), jrey@uemc.es (J.M. Rey-Hernández), eloy@eii.uva.es (E. Velasco Gómez), richard.gaggioli@marquette.edu (R. Gaggioli).

Peer review under responsibility of Faculty of Engineering, Alexandria University.

https://doi.org/10.1016/j.aej.2021.09.065

Nomenclature

c	specific heat, $J \cdot kg^{-1}\ K^{-1}$
d	prototype width, m
e	specific exergy, $kJ \cdot kg^{-1}$
$\dot{E}$	exergy flow, $kJ \cdot h^{-1}$
h	enthalpy, $kJ \cdot kg^{-1}$
H	prototype height, m
L	prototype length, m
"N"	narrow plates
s	entropy, $kJ \cdot kg^{-1}\ K^{-1}$
p	pressure, bar
Q	volume flow, $m^3 \cdot h^{-1}$
R	universal gas constant, $kJ \cdot kg^{-1}\ K^{-1}$
t	plate thickness, mm
T	temperature, °C
w	specific humidity, $g \cdot kg^{-1}$
"W"	wide plates

Greek symbols

ϕ	relative humidity
ε	exergetic efficiency

Subscripts and superscripts

0	environment
1	primary inlet
a	dry air
CH	chemical
D	destruction
F	fuel
in	inlet
L	loss
ma	moist air
out	outlet
p	pressure
P	product
PH	physical
v	vapour
w	liquid water

Acronyms:

AHU	Air Handling Unit
HP	Heat Pump
HVAC	Heating, Ventilation and Air Conditioning
IAPWS	International Association for the Properties of Water and Steam
IAQ	Indoor Air Quality
IEC	Indirect Evaporative Cooler
PVC	Polyvinyl Chloride
WBD	Wet Bulb Depression

Ministry of Industry considers that approximately 20% of the energy consumed in buildings could be saved.

Three proposals, in order to reduce the energy consumption in buildings, are given by Rey et al. [1]: 1) the decrease of the energy demand; 2) the replacement of traditional fossil energy sources with sustainable energy sources, and 3) the optimization of the processes energy utilization, with, for example, residual energy recovery. This work is related to alternative air-conditioning processes dealing with all these three procedures: 1) energy demand recovery; 2) free energy resources reutilization by means of energy recovery and evaporative cooling systems, and 3) energy efficiency optimization of the systems with the specification of their optimum configuration.

Evaporative cooling is a natural phenomenon that spontaneously occurs when water comes into contact with non-saturated air, hence in numerous examples in nature [2] (such as the sea breeze, after a summer storm or when sweat evaporates from our skin. Consequently, systems based on this effect are simple, energy efficient technologies. Although optimum efficiencies can be expected under hot and dry conditions [3,4] they are used in almost all climates [5]. Indeed, configurations such as indirect evaporative cooling, particularly in heat recovery mode, can enhance its application even in temperate climates [6]. Besides, hybrid systems with indirect evaporative cooling to precool air arise as a solution to achieve thermal comfort while lessening emissions, in a framework of increasing cooling demand due to a global warming situation to be restrained [7–9].

Exergy is widely accepted as the basis for defining efficiencies, as inefficiencies are a consequence of destruction or loss of available energy within the device [10]. Evaporative cooling has been studied from an exergetic point of view by several authors along the years. Already in 1979, Wepfer et al. [10] presented the proper evaluation of available energy for HVAC. Their main concepts have been applied to this work, with some important modifications related to the definition of the exergetic efficiency. Bejan [11] proposed in his book a general methodology for exergy analysis, with application to air conditioning processes. Ren et al. [12] presented the principles of exergy analysis in HVAC and the evaluation of evaporative cooling schemes. They suggested an unusual selection of the dead state. Some of their ideas have been applied in our paper. Qureshi and Zubair [13] applied exergy analysis to various psychrometric processes, evaporative cooling among them, to quantify the irreversible losses. Alhazmi [14] estimate the minimum work required for the air conditioning process. Taufiq et al. [15] used exergy analysis to evaluate overall and component efficiencies and to identify thermodynamic losses in an evaporative cooling system of a building in Malaysian climate. Caliskan et al. [16] presented energy and exergy analyses of one novel and three conventional types of air cooling systems for building applications, where they analyzed the effect of dead state temperature on specific exergy flow calculations.

Farmahini-Farahani et al. [17] applied exergy analysis to calculate the exergy efficiency of experimental investigations on the direct, indirect, and two stage indirect/direct evaporative cooling under various weather conditions. Ratlamwala and Dincer [18] defined energy and exergy efficiencies for evaporative cooling based on three different types of approaches. Santos et al. [19] presented a study on the performance of

the evaporative cooling process in air washes using exergy equations; they also obtained the conditions required for optimum performance with minimal exergy depletion. Uckan et al. [20] presented the exergy analysis of a novel configuration of a desiccant based evaporative air conditioning system, where the exergy destruction and the exergetic efficiency for all the components of the system -an evaporative cooler among themwere evaluated. Enteria et al. [21] developed a desiccant evaporative air-conditioning system and they evaluated it by an exergetic method under controlled environmental conditions to determine the performance of the whole system and its components. Elgendy et al. [22] proposed three novel desiccant evaporative cooling system configurations using direct/indirect evaporative cooler and they compared them by both energetic and exergetic analysis. In 2016 Ghazikhani et al. [23] performed an exergy analysis of two humidification process methods (constant enthalpy humidification and constant temperature humidification) in air conditioning systems. Sachdeva et al. [24] presented an energy and exergy analysis of an experimental direct evaporative cooling system. Also in 2016, Cuce and Riffat [25] performed a state of the art review of evaporative cooling systems for building applications, where, according to Kanoglu et al. [26] they emphasized that an exergy analysis needs to be considered for a through thermodynamic performance analysis of evaporative cooling systems. Some studies focus on the exergetic performance of hybrid Indirect Evaporative Cooling (IEC) and conventional air conditioning systems. Just recently, and based on mathematical models, Rao and Datta, [27] performed an exergy analysis of multihybrid evaporative cooling systems for different locations across India and evaluated their exergetic efficiency. Li et al. [28] studied an indirect evaporative cooler applied as an exhaust air heat recovery component using an exergy transfer model. Yang et al. [29] presented an energy and exergy analysis of five external-cooling evaporative coolers combined with mechanical vapor compression systems. But, it is important to underline the lack of exergy studies on experimental evaporative cooling systems in the literature.

In this paper, two experimental prototypes consisting of indirect evaporative cooling systems of different manufacturing characteristics have been analyzed through the exergy analysis methodology. Thus, with a thorough approach, we fill the existing gap in the literature with respect to the exergetic analysis of experimental evaporative cooling systems. First, in a previous paper [30], both prototypes were experimentally characterized. The prototypes have been designed and manufactured by the Thermal Engineering Group of the University of Valladolid. These two equally-sized cross-flow heat exchanger prototypes are made of polycarbonate hollow panels of different cross section, with a total heat exchange area of 6 m^2 and 3 m^2 respectively. They are connected into a heat-recovery cycle within a whole experimental setup constructed for the tests. Each prototype has been tested at 4 levels of outdoor air volume flow (125, 200, 300 and 400 $m^3 \cdot h^{-1}$) and 4 levels of dry bulb temperature (from 25 to 40 °C). Next, the results are studied considering the influence of construction aspects, outdoor air flow and temperature on the energy performance. The exergy destructed by each prototype in the 16 different operating conditions has been calculated and the optimum combination of operating conditions has been proposed.

2. Materials: Experimental setup

To improve energy efficiency when supplying the required ventilation demand, a plastic plate heat exchanger is designed for energy recovery combined with evaporative cooling.

Compared to metallic materials, the use of plastic in indirect evaporative coolings has the advantage of being lighter, cheaper and, above all, corrosion resistant. Its lower thermal conductivity can be overcome using thin plates: because thermal resistance to conduction in plates is proportional to the plate thickness and indirectly proportional to its conductivity, small thicknesses make convection the dominating resistance to heat transfer [31,32]. This is the reason why, since several decades ago, many indirect evaporative coolers are being built in plastic [33–36].

Two prototypes, called "W" (wide plates) and "N" (narrow plates), have been built made of 15 and 28 polycarbonate hollow plates respectively, of two different thickness. The dimensions and total heat exchange area of both prototypes can be identified in Fig. 1 and Table 1.

As shown in Fig. 1, the prototypes have a crossflow configuration. Primary outdoor air flows within the plates and traverses the device in the L direction, while secondary air flows upwards inside the plates. Water is supplied inside the plates in counterflow to air, from an upper water distributor.

A PVC structure serves as the shell of the prototypes and enables their connection through air ducts to an Air Handling Unit (AHU) and a climate test room, as shown in Fig. 2 and Fig. 3. The test rig has a water circuit consisting of a water distributor, a tank, a water pump and the required ducts.

As shown in Fig. 3, the prototypes operate in a heat-recovery mode. Primary air from the AHU flows through the space between the plates. The AHU provides the primary airflow in the outdoor conditions to be tested. This primary air is cooled due to the indirect contact with the secondary, return airflow coming from the climate test room. A heat

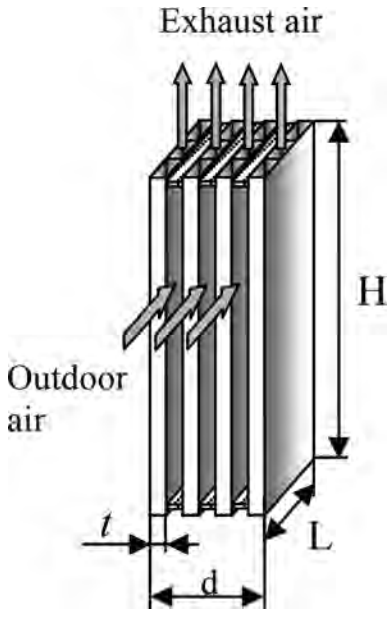

Fig. 1 Configuration of the prototypes.

Table 1 Dimensions and configuration of the prototypes..

	Type W	Type N
Number of plates	15	28
Height H	0.62 m	0.62 m
Length L	0.18 m	0.18 m
Width d	0.23 m	0.23 m
Total exchange area	3 m^2	5.6 m^2
Polycarbonate wall thickness	0.1 mm	0.1 mm
Panel thickness t	9 mm	4 mm

pump inside the climate chamber provides additional cooling to achieve comfort, when required. 16 tests have been conducted for each prototype, hence a total of 32 tests, varying both the primary air flow and dry bulb temperature in the AHU. Tests are performed at four levels of primary air volume flow (125, 200, 300 and 400 $m^3 \cdot h^{-1}$) and four levels of dry bulb temperature (25, 30, 35 and 40 °C). Conditions of secondary air are those of thermal comfort maintained inside the space (dry bulb temperature 22 ± 0.5 °C and relative humidity between 50 and 65%). Water mass flow is supplied at a constant rate of 0.14 kg/s for all tests and its temperature maintains at that of wet bulb of the secondary air stream (between 18 and 19.5 °C).

During the tests, inlet air volume flow and dry bulb temperature varied slightly from the set conditions. Standard deviation of the measured air temperatures at the inlet ranged from 0.15 °C to 0.37 °C, while that of the measured air volume flow ranged from 0.9 m^3/h to 6.4 m^3/h.

During the tests, dry bulb temperature and relative humidity have been measured at the inlet and outlet of both airflows (Fig. 3). Temperature probes are 4-wire Pt100 (accuracy: ±0.1 °C, range: −50 to 250 ^{0}C) and relative Humidity probes are capacitive sensors (accuracy: ±2%, range: 0 to 100%). Volume airflows are obtained through the pressure drop generated in orifice plates, measured with ultra-low differential pressure transmitters of pressure range 0 mm to 703.1 mm H_2O and accuracy ± 2%. The orifice plates are calibrated with an airflow nozzle.

3. Methods: Exergy analysis

The method of exergy analysis enables the cause and true magnitude of the inefficiencies in a process or energy system. Exergy is the maximum theoretical useful work obtainable as the system interacts with the reference environment to equilibrium [37]. Therefore, the value assigned to the exergy of a material stream depends upon the proper selection of the reference environment. Once the equilibrium is achieved, the system is in the so called dead state. The fundamental dead state is that state which would be attained if each constituent of the substance were reduced to complete equilibrium with the stable components in the environment [10]. At the dead state, the pressure, temperature and chemical potentials of the system equals those of the environment. There is no standard reference; the appropriate reference depends upon the process and the system being analyzed and upon the ambient environment.

Usually, the appropriate dead state temperature, T_0, is the ambient dry-bulb temperature. In our study the temperature of the environment is not always the same. Four levels of dry bulb temperature have been considered. Therefore, as the dead state temperature we have taken the correspondent temperature of the environment for each set of experiments (from 25 to 40 °C). The dead state pressure is the barometric pressure, in our case p_0 = 92.6 kPa. Related to the reference humidity, several options are considered in the literature: Wepfer et al. [10] take w_0 as the outdoor value at that instant; Liley [38] established the conditions of dry air, Φ_0 = 0; Bejan [11] assume a standard relative humidity of Φ_0 = 60 %; Uckan [20] used the daily mean specific humidity ratio value of ambient air; Ren et al. [12,39] considered Φ_0 = 100 %, since the water vapor can diffuse into air as long as the air does not reach the saturation at a given temperature and pressure. Taking into account that the definition of exergy assumes the interaction of the system with the environment to equilibrium, it seems to be more convenient to choose the outdoor humidity as the dead state value, that is Wepfer et al. argument. This approach is used in this paper.

The specific exergy flow of moist-air may be defined as [10]:

$$e_{ma} = (c_{p,a} + w c_{p,v}) T_0 \left(\frac{T}{T_0} - 1 - \ln \frac{T}{T_0} \right) + (1 + w) R_a T_0 \ln \frac{p}{p_0} + R_a T_0 \left[(1 + w) \ln \frac{(1 + w_0)}{(1 + w)} + w \ln \frac{w}{w_0} \right] \quad (1)$$

where the first two terms of this expression refer to the physical exergy and the last term to the chemical exergy. In this study, the following values of the parameters have been used: c_{pa} = 1.

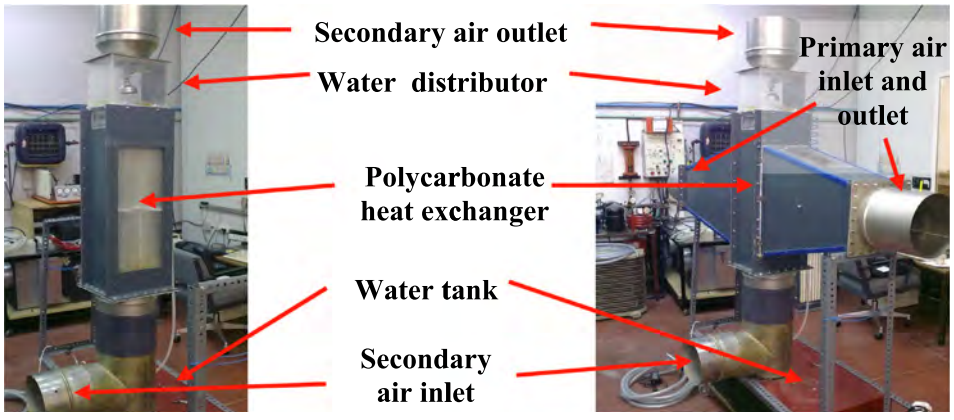

Fig. 2 View of the prototype, the shell and the assembly.

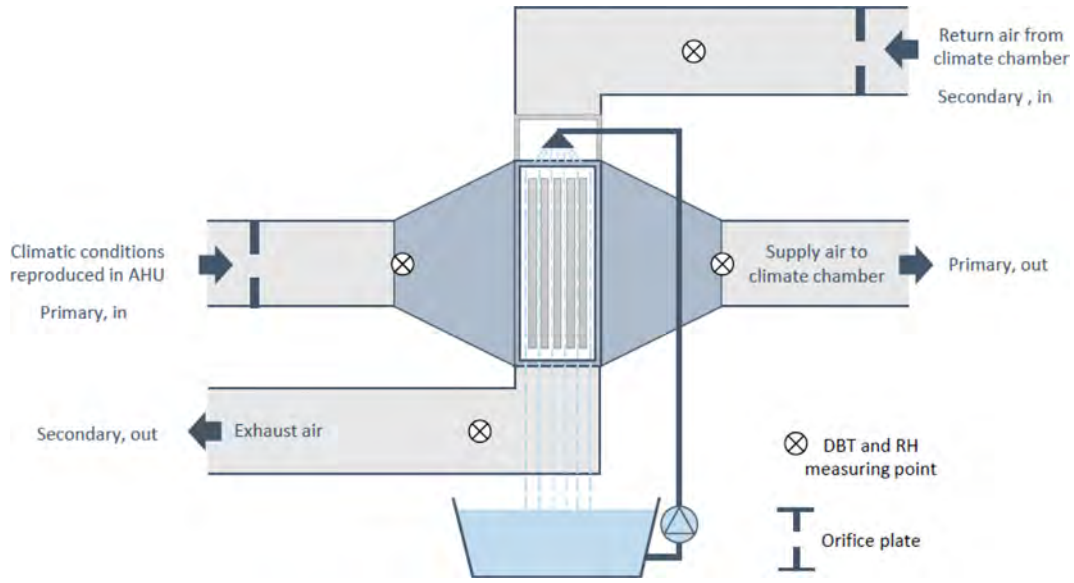

Fig. 3 Scheme of the experimental setup.

003 kJ·kg^{-1}K^{-1}, c_{pv} = 1.872 kJ·kg^{-1}K^{-1}, R_a = 0.287 kJ·kg^{-1}K^{-1}and $w = 1.608w$.

And the specific exergy flow of liquid water is given by:

$$e_{H_2O} = h_w(T,p) - h_{w,0}\left(T_0, p_{w,0}\right) - T_0\left[s_w(T,p) - s_{w,0}\left(T_0, p_{w,0}\right)\right] \quad (2)$$

where the corresponding enthalpy and entropy values have been taken from [40]. This formulation takes into account that, at the final equilibrium state, the water will be one of the constituents of an ideal mixture, that is the outdoor wet air. Therefore, both the physical and the chemical contributions to the exergy value of liquid water, are already included in Eq. (2).

The exergetic efficiency measures the true thermodynamic efficiency of a process. It is defined by [37]:

$$\varepsilon = \frac{\dot{E}_P}{\dot{E}_F} \quad (3)$$

Where the exergy of the product, $\dot{E}_P$, consist of the exergy of the energy streams generated in the component plus all the exergy increases between inlet and outlet that are in accord with the purpose of the component. Concerning the exergy of the fuel, $\dot{E}_F$, it is the sum of the exergy of the energy streams supplied to the component plus all the exergy decreases between inlet and outlet and the exergy increases (between inlet and outlet) that are not in accord with the purpose of the component [41].

The purpose of our evaporative cooler with heat recovery is to decrease the temperature of the primary air, while the humidity of the secondary air increases and its temperature decreases. As the heat transfer occurs below T_0, exergy is transferred in the direction opposite to the heat transfer [37]. Therefore, the exergy supplied by the water, the pump and the secondary air stream is used to increase the exergy of the primary stream. This means that the appropriate definitions of exergy of the fuel and exergy of the product for this device are following:

$$\dot{E}_P = \dot{E}_{primary,\ out} \quad (4)$$

$$\dot{E}_F = \Delta\dot{E}_{supplied,\ H_2O} + \dot{W}_{pump} + \dot{E}_{secondary,\ in} \quad (5)$$

The exergy destruction can be obtained through the simple balance:

$$\dot{E}_D = \dot{E}_F - \dot{E}_P - \dot{E}_L \quad (6)$$

where $\dot{E}_L = \dot{E}_{secondary,out}$ because this flow material is released into the atmosphere.

4. Results and discussion

The results of the specific exergy flows are presented in Table 2 for both prototypes "W" (wide-plates) and "N" (narrow-plates). For each inlet and outlet streams of the primary and secondary air-flows, the volume flow, Q, the dry-bulb temperature, T, the humidity, w, and the calculated values for the physical, e^{PH}, and the chemical exergies, e^{CH}, are listed.

Table 3 contains the results of the exergetic analysis for both prototypes –wide and narrow- at the different experimental conditions: the four levels of primary air volume flow (125, 200, 300 and 400 m^3·h^{-1}) and four levels of dry bulb temperature (from 25 to 40 °C). For each of the 16 tests, the exergy of the fuel, $\dot{E}_F$, the exergy of the product, $\dot{E}_P$, the exergy destruction, $\dot{E}_D$, and the exergetic efficiency, ε, have been calculated.

At first sight, Table 3 shows that the exergetic efficiency of this device, no matter the operation conditions, is very low (2–12 %). The high internal irreversibilities, due to heat transfer and diffusion, the exergy losses into the atmosphere, and the low exergetic value of the primary outlet stream are the reason of these low exergetic efficiency values.

Fig. 4 shows an exergy flow diagram for the prototype "N" with a 200 $m^3{\cdot}h^{-1}$ operating flow. The high exergy destruction becomes evident, as well as the losses. Therefore, the exergy of the product is very small.

Table 2 Results of the specific exergy flows for prototypes "W" and "N".

Primary air-flow inlet					*Primary air-flow outlet*				*Secondary air-flow inlet*					*Secondary air-flow outlet*			
Q $m^3 \cdot h^{-1}$	T °C	w $g \cdot kg^{-1}$	e^{PH} $kJ \cdot kg^{-1}$	e^{CH} $kJ \cdot kg^{-1}$	T °C	w $g \cdot kg^{-1}$	e^{PH} $kJ \cdot kg^{-1}$	e^{CH} $kJ \cdot kg^{-1}$	Q $m^3 \cdot h^{-1}$	T °C	w $g \cdot kg^{-1}$	e^{PH} $kJ \cdot kg^{-1}$	e^{CH} $kJ \cdot kg^{-1}$	T °C	w $g \cdot kg^{-1}$	e^{PH} $kJ \cdot kg^{-1}$	e^{CH} $kJ \cdot kg^{-1}$
Type "W"																	
400	40	9.07	0.000	0.000	32.2	9.07	0.119	0.000	156.1	20.7	7.0	0.680	0.036	18.9	16.02	0.809	0.308
	35	8.91	0.000	0.000	29.0	8.91	0.075	0.000	187.1	21.5	8.0	0.343	0.007	18.5	15.80	0.506	0.302
	30	8.12	0.000	0.000	25.5	8.12	0.042	0.000	134.2	22.4	7.3	0.110	0.006	17.4	14.57	0.293	0.285
	25	8.46	0.000	0.000	22.4	8.46	0.017	0.000	127.8	22.7	7.9	0.014	0.002	17.0	14.53	0.126	0.243
300	40	9.73	0.000	0.000	31.2	9.73	0.142	0.000	133.2	21.8	8.4	0.591	0.015	18.8	16.29	0.801	0.260
	35	9.01	0.000	0.000	28.0	9.01	0.088	0.000	128.0	22.3	7.9	0.284	0.011	18.1	15.56	0.505	0.272
	30	8.49	0.000	0.000	24.9	8.49	0.052	0.000	129.2	23.4	7.9	0.084	0.003	17.4	14.96	0.294	0.276
	25	8.67	0.000	0.000	21.9	8.67	0.021	0.000	129.5	22.7	8.1	0.013	0.002	16.8	14.36	0.132	0.211
200	40	10.09	0.000	0.000	30.2	10.09	0.174	0.000	132.9	22.0	8.8	0.576	0.013	19.1	16.68	0.778	0.256
	35	9.93	0.000	0.000	27.5	9.93	0.104	0.000	139.3	22.1	9.0	0.300	0.006	18.5	16.15	0.489	0.228
	30	7.52	0.000	0.000	24.2	7.52	0.062	0.000	139.9	22.1	6.8	0.114	0.005	16.3	13.57	0.333	0.269
	25	7.68	0.000	0.000	21.7	7.68	0.030	0.000	131.9	22.2	7.2	0.022	0.002	16.1	13.51	0.166	0.244
125	40	8.77	0.000	0.000	28.1	8.77	0.232	0.000	130.2	23.4	7.4	0.457	0.015	17.6	14.84	0.849	0.247
	35	7.95	0.000	0.000	25.4	7.95	0.156	0.000	134.2	22.7	6.9	0.257	0.010	16.5	13.69	0.594	0.238
	30	7.40	0.000	0.000	23.0	7.40	0.087	0.000	138.4	22.6	6.7	0.099	0.005	16.1	13.14	0.344	0.249
	25	7.50	0.000	0.000	21.2	7.50	0.030	0.000	129.3	23.7	7.2	0.005	0.001	16.9	13.66	0.125	0.275
Type "N"																	
400	40	8.04	0.000	0.000	34.3	8.4	0.058	0.000	28.7	21.6	6.7	0.588	0.016	23.6	22.68	0.464	1.260
	35	7.38	0.000	0.000	30.7	7.7	0.035	0.000	26.6	21.6	6.4	0.319	0.009	22.2	20.81	0.292	1.138
	30	7.01	0.000	0.000	27.4	7.3	0.020	0.000	25.6	21.5	6.4	0.149	0.004	20.9	19.27	0.169	0.996
	25	6.69	0.000	0.000	23.3	7.0	0.008	0.000	25.3	22.4	6.4	0.017	0.001	19.2	17.36	0.069	0.799
300	40	7.97	0.000	0.000	33.6	8.2	0.079	0.000	26.1	21.6	6.8	0.604	0.013	23.9	22.60	0.467	1.269
	35	7.60	0.000	0.000	30.8	7.9	0.039	0.000	24.8	21.7	6.8	0.332	0.007	23.8	22.65	0.239	1.352
	30	6.72	0.000	0.000	25.8	6.9	0.042	0.000	37.1	22.3	6.2	0.123	0.003	18.5	16.36	0.260	0.680
	25	6.57	0.000	0.000	22.9	6.8	0.013	0.000	26.7	22.4	6.3	0.018	0.001	19.0	16.96	0.078	0.774
200	40	7.96	0.000	0.000	31.3	8.0	0.143	0.000	34.2	21.9	6.8	0.587	0.013	21.4	18.84	0.624	0.762
	35	7.29	0.000	0.000	28.0	7.4	0.100	0.000	43.9	22.3	6.4	0.308	0.009	19.0	15.25	0.477	0.462
	30	7.28	0.000	0.000	24.7	7.4	0.060	0.000	45.7	22.8	6.7	0.105	0.003	17.7	14.62	0.287	0.394
	25	6.71	0.000	0.000	21.3	6.9	0.027	0.000	52.2	21.2	6.4	0.028	0.001	16.3	13.29	0.139	0.340
125	40	9.41	0.000	0.000	29.2	8.9	0.222	0.000	131.7	23.7	8.0	0.487	0.015	19.2	15.83	0.786	0.258
	35	8.13	0.000	0.000	26.2	7.9	0.155	0.000	85.8	21.7	7.1	0.341	0.010	17.5	14.16	0.576	0.256
	30	8.00	0.000	0.000	23.9	8.0	0.067	0.000	82.6	23.3	7.4	0.081	0.003	17.3	14.04	0.288	0.256
	25	7.44	0.000	0.000	21.2	7.6	0.027	0.000	77.0	21.9	7.0	0.019	0.002	16.3	13.27	0.136	0.250

Table 3 Results of the exergy analysis for both prototypes.

Q	T	*Type "W"*					*Type "N"*				
		$\dot{E}_F$	$\dot{E}_P$	$\dot{E}_D$	$\dot{E}_L$	ε	$\dot{E}_F$	$\dot{E}_P$	$\dot{E}_D$	$\dot{E}_L$	ε
$m^3 \cdot h^{-1}$	°C	$kJ \cdot h^{-1}$	$kJ \cdot h^{-1}$	$kJ \cdot h^{-1}$	$kJ \cdot h^{-1}$	%	$kJ \cdot h^{-1}$	$kJ \cdot h^{-1}$	$kJ \cdot h^{-1}$	$kJ \cdot h^{-1}$	%
400	40	612.60	47.99	370.06	194.55	7.8	244.25	23.20	165.91	55.14	9,5
	35	508.05	29.57	310.52	167.96	5.8	198.62	13.73	142.39	42.50	6,9
	30	301.88	16.30	199.32	86.26	5.4	166.97	7.56	126.15	33.26	4,5
	25	213.34	6.69	154.45	52.20	3.1	138.30	3.20	110.63	24.47	2,3
300	40	463.50	42.23	264.60	156.67	9.1	230.77	23.43	156.90	50.44	10,2
	35	356.88	25.88	220.69	110.31	7.3	200.38	11.32	145.05	44.01	5,6
	30	276.60	15.08	179.94	81.58	5.5	181.03	12.31	129.82	38.90	6,8
	25	204.80	6.14	149.55	49.11	3.0	140.93	3.64	111.96	25.33	2,6
200	40	450.46	37.05	261.48	151.93	8.2	236.24	28.33	155.04	52.87	12,0
	35	351.25	21.85	218.97	110.43	6.2	208.57	19.80	142.75	46.02	9,5
	30	307.16	12.65	200.59	93.92	4.1	172.17	11.95	125.57	34.65	6,9
	25	227.65	6.02	161.49	60.14	2.6	153.88	5.28	120.74	27.86	3,4
125	40	425.46	25.92	241.33	158.21	6.1	445.93	27.82	266.09	152.02	6,2
	35	352.78	17.55	211.11	124.12	5.0	276.02	19.48	177.04	79.50	7,1
	30	293.72	10.81	191.65	91.26	3.7	205.64	8.29	147.45	49.90	4,0
	25	223.92	4.05	162.37	57.50	1.8	167.70	3.25	131.36	33.09	1,9

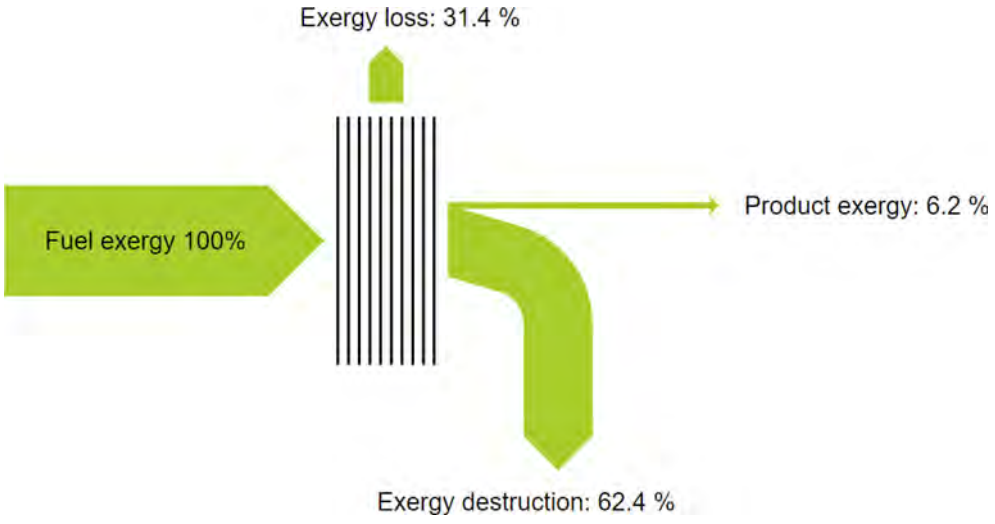

Fig. 4 Exergy flow diagram of the evaporative cooler, prototype "N" with a flow rate of $200 m^3 h^{-1}$.

Related to the trend, followed along the different experiments, the available fuel exergy decreases as primary inlet temperature decreases, as expected. The same trend is followed by the exergy of the product, the exergy destruction, and the exergy losses; as a result, the exergetic efficiency also diminishes. Primary air volume flow decrease also involves a decrease in the exergy of the fuel and the exergy of the product and, therefore, an exergy destruction decrease for both prototypes. Nevertheless, this effect is not that remarkable on the exergetic efficiency of the device. Generally, higher results are observed in exergy destruction when doubling the heat exchange area (facing prototype "N" to prototype "W"), but the exergetic efficiency seems not to be affected by the size of the panels' hollows. A better overview of the global tendency can be reached through the figures presented in the following section.

4.1. Analysis of the exergetic efficiency

To perform a comparison among all the related experiments, the relationship between the exergetic efficiency and the primary inlet temperature is presented in Fig. 5 a) for the prototype "W" and b) for the prototype "N".

The exergetic efficiency values, calculated using (3) are in the order of 2–12 %. In the prototype "W", the exergetic efficiency increases with the volume flow of the primary air, because an increase in the outdoor air volume flow improves the heat transfer [42]. This behavior is in agreement with the

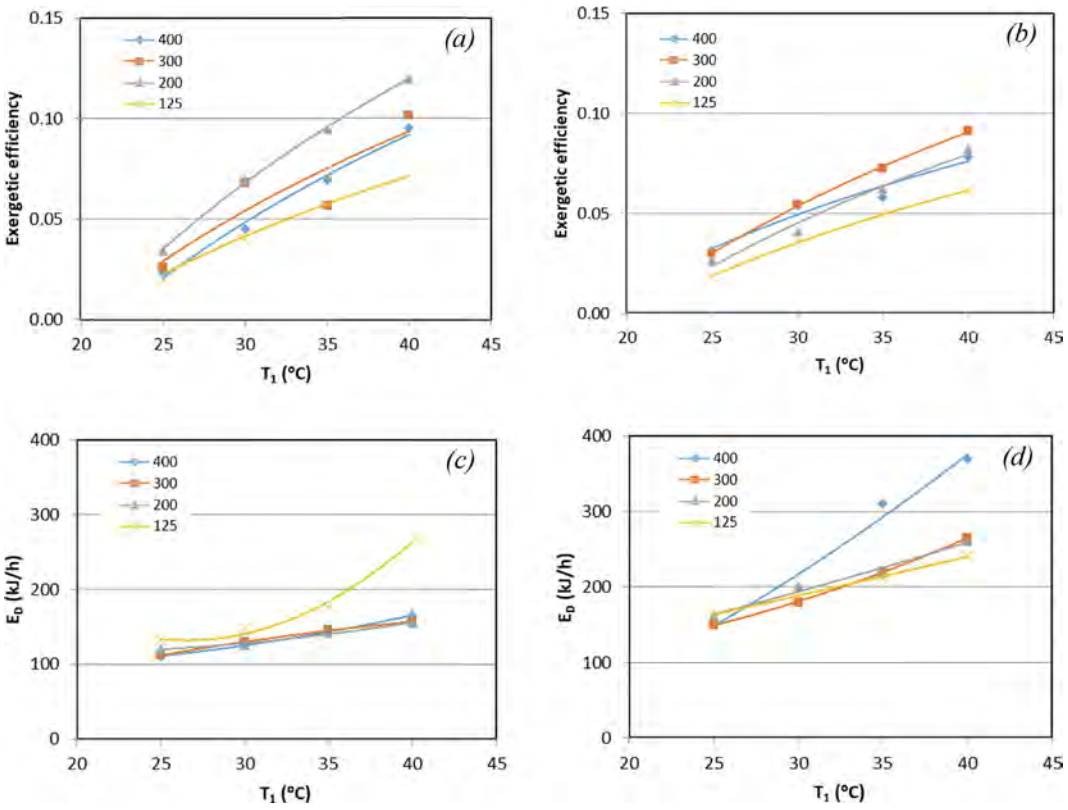

Fig. 5 Relationship between the exergetic efficiency and the exergy destruction with the primary inlet temperature for (a) and (c) prototype "W", (b) and (d) prototype "N".

improvement of the thermal conductance when higher airflows are tested, which could be due to convective coefficients improvement in the heat-exchanger primary air side, as concluded in a previous paper [42]. There are a couple of exceptions to this behavior: for example, 35 and 40 °C compared to the tests with the highest volume flow (400 $m^3 \cdot h^{-1}$) at high temperatures (35 and 40 °C) that present an exergetic efficiency lower than expected. This could be attributed to the increase of the inefficiencies due to turbulence. Looking at the secondary air Qs in Table 2, the flowrates are much higher at 35 and 40 °C than those at 25 and 30 (especially when compared with values and variations when the primary air flows are at 300, 200 and 125). So the secondary air exergy losses would be expected to be much higher and not surprisingly the destructions could also increased. As a result, for prototype "W", the optimal volume flow of the primary air seems to be 300 $m^3 \cdot h^{-1}$.

In the prototype "N", the highest exergetic efficiencies are associated with the volume flow of 200 $m^3 \cdot h^{-1}$ for the entire range of temperatures. For the tests related with the other volume flows, some deviations due to unidentified factors appear. Likewise, for Type N, the secondary Qs at 300 and 35, and at 125 and 40 °C are very high, comparatively.

On the other hand, the exergetic efficiency increases as the primary inlet temperature increases. This effect is more pronounced for the prototype "N". This can be due to the increase in the heat transfer as a consequence of the also higher temperature difference between both air streams. Just the tests related to 35 °C-300 $m^3 \cdot h^{-1}$, and 40 °C-125 $m^3 \cdot h^{-1}$, present exceptions to this behavior; but they can be more properly attributed to variability in operating conditions.

4.2. Analysis of the exergy destruction

Fig. 4 also shows the relationship between the exergy destruction and the primary inlet temperature, for c) prototype "W" and d) prototype "N".

The figure shows that the exergy destruction with prototype "W" is higher than with prototype "N". At first sight, the higher the inlet temperature of the primary air, the higher the exergy destruction for both prototypes. The trend followed with the variation of the volume flow is, on the contrary, not that clear. The results regarding 200, 300, and 400 $m^3 \cdot h^{-1}$ with both prototypes show that the volume flow of the primary air does not seem to have an important role. There are just a couple of protrudings in this figure, with high exergy destruction values. In prototype "W", at 35–40 °C of inlet temperature of the primary air and a control volume of 400 $m^3 \cdot h^{-1}$, a disproportionate high value of the exergy destruction could be attributed to the increase of inefficiencies due to turbulence, as mentioned before. In prototype "N", the exergy destructed when a primary air volume flow of 125 $m^3 \cdot h^{-1}$ was used is clearly higher than when the other volume flows were tested, for the whole range of temperatures, and with an outstanding exergy destruction value for 40 °C. but this could be due to the instabilities observed in this operating conditions.

Fig. 6 shows the correlation between the exergetic efficiency and the Wet Bulb Depression (WBD) (the difference between the dry bulb temperature and its coincident wet bulb temperature). The interest of this parameter in evaporative cooling applications was previously appointed in the literature [43].

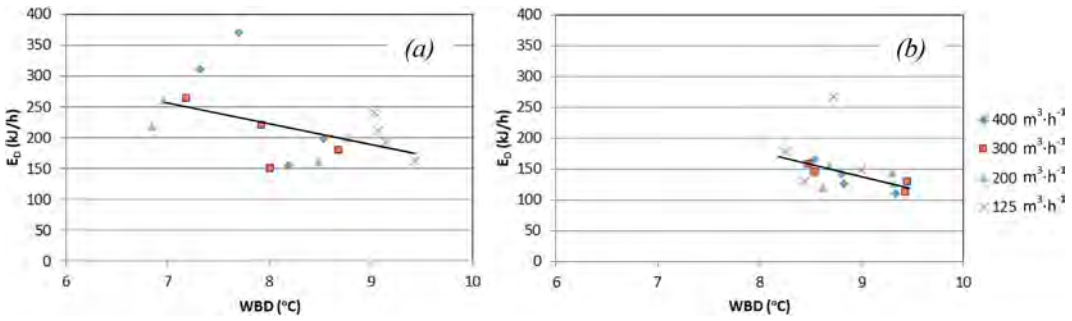

Fig. 6 Relationship between the exergetic efficiency and the Wet Bulb Depression for (a) prototype "W" and (b) prototype "N".

In our study WBD of the secondary air inlet has been considered.

Although the dispersion of the results is high, especially for prototype "W", some interesting conclusions could be performed. The clear tendency (represented by a straight line in both figures) is that the lower the wet bulb depression temperature, the higher the exergy destruction. This tendency agrees with the increase in temperature drops with the WBD which leads to more efficient situations.

5. Conclusions

In this work, two experimental indirect evaporative cooling prototypes, made of polycarbonate hollow panels, have been analyzed through the exergy analysis methodology. The prototypes operate in a heat-recovery mode. Different operating conditions have been tested: 4 levels of outdoor air volume flow (125, 200, 300 and 400 $m^3 \cdot h^{-1}$) and 4 levels of dry bulb temperature (from 25 to 40 °C).

Generally, exergy destruction increases when doubling the heat exchange area. For both prototypes, the higher the dry bulb temperature at the inlet of the primary air, the higher the exergy destruction and the exergy losses. The effect of the increase of the volume flow of the primary air is not always that clear. In general, a primary air volume flow reduction also implies an exergy destruction decrease for both prototypes, but some uncertainties have been observed due to variability in the operating conditions. It has also been appreciated that the exergy destruction increases when the wet bulb depression temperature of the secondary air inlet decreases, leading to more inefficient configurations.

The value of the exergetic efficiency is in the order of 2–12 %, which seems to be pretty low. So, in this case, an exergy costing analysis is highly recommended, in order to analyse the economic performance of the device. The wider the hollow plates, the lower the exergetic efficiency of the prototype. This value clearly increases with the primary inlet temperature; the trend with the volume flow of the primary air is not that obvious. It is supposed that an increase in the outdoor air volume flow improves heat transfer and, hence, the exergetic efficiency. This tendency is clearly followed by prototype "W"; on the contrary, in the prototype "N", the highest exergetic efficiencies are associated with the volume flow of 200 $m^3 \cdot h^{-1}$ for the entire range of temperatures.

The overall results show that "N" is the most efficient prototype. The optimum volume flow operating conditions for each prototype at any inlet temperature of the primary air can be proposed as: 300 $m^3 \cdot h^{-1}$. for the "W" prototype, 200 $m^3 \cdot h^{-1}$. for the "N prototype. The higher the outdoor temperature operation conditions, the higher the efficiency for both prototypes.

Indirect evaporative cooling can reduce the energy consumed by conventional vapor compression air conditioning systems. Further research on the global exergy efficiency of hybrid systems can provide additional insight on the improvements achieved by precooling air through IEC.

CRediT authorship contribution statement

Ana M. Blanco-Marigorta: Conceptualization, Formal analysis, Funding acquisition, Software, Methodology, Visualization, Writing – original draft. **Ana Tejero-González:** Conceptualization, Data curation, Investigation, Visualization, Writing – original draft. **Javier M. Rey-Hernández:** Data curation, Investigation, Validation. **Eloy Velasco Gómez:** Conceptualization, Data curation, Investigation, Resources, Supervision, Writing – review & editing. **Richard Gaggioli:** Methodology.

Declaration of Competing Interest

The authors declare that they have no known competing financial interests or personal relationships that could have appeared to influence the work reported in this paper.

Acknowledgements

This research has been co-funded by ERDF funds, INTERREG MAC 2014-2020 programme, within the ACLIEMAC project (MAC2/3.5b/380). No funding sources had any influence on study design, collection, analysis, or interpretation of data, manuscript preparation, or the decision to submit for publication.

References

[1] F.J. Rey Martínez, J.F. San José Alonso, E. Velasco Gómez, Á.-G. Plasencia, M.A., Recuperación de energía en sistemas de climatización. Documentos Técnicos de Instalaciones en la Edificación, DTIE 8.01, El Instalador, Madrid, Spain, 2000.

[2] J.R. Watt, Evaporative Air Conditioning Handbook, 2nd ed., Chapman & Hall, New York, 1986.

[3] G.P. Maheshwari, F. Al-Ragom, R.K. Suri, Energy-saving potential of an indirect evaporative cooler, Appl. Energy. 69 (2001) 69–76, https://doi.org/10.1016/S0306-2619(00)00066-0.
[4] S.S. Chauhan, S.P.S. Rajput, Parametric analysis of a combined dew point evaporative-vapour compression based air conditioning system, Alexandria Eng. J. 55 (2016) 2333–2344, https://doi.org/10.1016/j.aej.2016.05.005.
[5] ASHRAE. 2019 ASHRAE Handbook–HVAC Applications., American Society of Heating, Refrigerating and Air-Conditioning Engineers, Atlanta, 2019.
[6] D. Pandelidis, A. Cichoń, A. Pacak, S. Anisimov, P. Drąg, Counter-flow indirect evaporative cooler for heat recovery in the temperate climate, Energy 165 (2018) 877–894, https://doi.org/10.1016/j.energy.2018.09.123.
[7] C. X., S. L., Y. W., Z. S., J. L., M. X., Studying the Performance of an Indirect Evaporative Pre-cooling System in Humid Tropical Climates, in: L.J. Wang Z., Zhu Y., Wang F., Wang P., Shen C. (Ed.), Proc. 11th Int. Symp. Heating, Vent. Air Cond. (ISHVAC 2019). ISHVAC 2019. Environ. Sci. Eng., Springer, Singapore, 2020. Doi: 10.1007/978-981-13-9524-6_49.
[8] Y. Al-Horr, B. Tashtoush, N. Chilengwe, M. Musthafa, Performance assessment of a hybrid vapor compression and evaporative cooling fresh-air-handling unit operating in hot climates, Processes 7 (2019), https://doi.org/10.3390/pr7120872.
[9] A.E. Kabeel, M. Abdelgaied, R. Sathyamurthy, T. Arunkumar, Performance improvement of a hybrid air conditioning system using the indirect evaporative cooler with internal baffles as a pre-cooling unit, Alexandria Eng. J. 56 (2017) 395–403, https://doi.org/10.1016/j.aej.2017.04.005.
[10] W.J. Wepfer, R.A. Gaggioli, E.F. Obert, Proper evaluation of available energy for HVAC, ASHRAE Trans. 85 (1) (1979) 214–230.
[11] A. Bejan, Advanced engineering thermodynamics, 2nd ed., Wiley, New York, 1988.
[12] R. Chengqin, L. Nianping, T. Guangfa, Principles of exergy analysis in HVAC and evaluation of evaporative cooling schemes, Build. Environ. 37 (2002) 1045–1055, https://doi.org/10.1016/S0360-1323(01)00104-4.
[13] B.A. Qureshi, S.M. Zubair, Application of exergy analysis to various psychrometric processes, Int. J. Energy Res. 27 (2003) 1079–1094, https://doi.org/10.1002/er.933.
[14] M.M. Alhazmy, The minimum work required for air conditioning process, Energy. 31 (2006) 2403–2413, https://doi.org/10.1016/j.energy.2005.12.007.
[15] B.N. Taufiq, H.H. Masjuki, T.M.I. Mahlia, M.A. Amalina, M. S. Faizul, R. Saidur, Exergy analysis of evaporative cooling for reducing energy use in a Malaysian building, Desalination 209 (2007) 238–243, https://doi.org/10.1016/j.desal.2007.04.033.
[16] H. Caliskan, I. Dincer, A. Hepbasli, Exergetic and sustainability performance comparison of novel and conventional air cooling systems for building applications, Energy Build. 43 (2011) 1461–1472, https://doi.org/10.1016/j.enbuild.2011.02.006.
[17] M. Farmahini-Farahani, S. Delfani, J. Esmaeelian, Exergy analysis of evaporative cooling to select the optimum system in diverse climates, Energy 40 (2012) 250–257, https://doi.org/10.1016/j.energy.2012.01.075.
[18] T.A.H. Ratlamwala, I. Dincer, Efficiency assessment of key psychometric processes, Int. J. Refrig. 36 (2013) 1142–1153, https://doi.org/10.1016/j.ijrefrig.2012.10.038.
[19] J.C. Santos, G.D.T. Barros, J.M. Gurgel, F. Marcondes, Energy and exergy analysis applied to the evaporative cooling process in air washers, Int. J. Refrig. 36 (2013) 1154–1161, https://doi.org/10.1016/j.ijrefrig.2012.12.012.
[20] I. Uçkan, T. Yilmaz, E. Hürdoğan, O. Büyükalaca, Exergy analysis of a novel configuration of desiccant based evaporative air conditioning system, Energy Convers. Manag. 84 (2014) 524–532, https://doi.org/10.1016/j.enconman.2014.05.006.
[21] N. Enteria, H. Yoshino, R. Takaki, A. Mochida, A. Satake, R. Yoshie, Effect of regeneration temperatures in the exergetic performances of the developed desiccant-evaporative air-conditioning system, Int. J. Refrig. 36 (2013) 2323–2342, https://doi.org/10.1016/j.ijrefrig.2013.08.005.
[22] E. Elgendy, A. Mostafa, M. Fatouh, Performance enhancement of a desiccant evaporative cooling system using direct/indirect evaporative cooler, Int. J. Refrig. 51 (2015) 77–87, https://doi.org/10.1016/j.ijrefrig.2014.12.009.
[23] M. Ghazikhani, I. Khazaee, S. Vahidifar, Exergy analysis of two humidification process methods in air-conditioning systems, Energy Build. 124 (2016) 129–140, https://doi.org/10.1016/j.enbuild.2016.04.077.
[24] A. Sachdeva, S.P.S. Rajput, A. Kothari, Energy and Exergy Analysis of Direct Evaporative Cooling, System 4 (2016) 1–6.
[25] P.M. Cuce, S. Riffat, A state of the art review of evaporative cooling systems for building applications, Renew. Sustain. Energy Rev. 54 (2016) 1240–1249, https://doi.org/10.1016/j.rser.2015.10.066.
[26] M. Kanoğlu, M.Ö. Çarpinlioğlu, M. Yildirim, Energy and exergy analyses of an experimental open-cycle desiccant cooling system, Appl. Therm. Eng. 24 (2004) 919–932, https://doi.org/10.1016/j.applthermaleng.2003.10.003.
[27] V.V. Rao, S.P. Datta, Comprehensive exergetic, sustainability and enviro-economic evaluation of single-stage and hybrid evaporative coolers in India, Sustain. Energy Technol. Assessments 47 (2021), https://doi.org/10.1016/j.seta.2021.101403 101403.
[28] W. Li, Y. Li, W. Shi, J. Lu, Energy and exergy study on indirect evaporative cooler used in exhaust air heat recovery, Energy 235 (2021), https://doi.org/10.1016/j.energy.2021.121319 121319.
[29] Y. Yang, C. Ren, C. Yang, M. Tu, B. Luo, J. Fu, Energy and exergy performance comparison of conventional, dew point and new external-cooling indirect evaporative coolers, Energy Convers. Manag. 230 (2021), https://doi.org/10.1016/j.enconman.2021.113824 113824.
[30] E. Velasco Gómez, A. Tejero González, F.J. Rey Martínez, Experimental characterisation of an indirect evaporative cooling prototype in two operating modes, Appl. Energy. 97 (2012) 340–346, https://doi.org/10.1016/j.apenergy.2011.12.065.
[31] C. T'Joen, Y. Park, Q. Wang, A. Sommers, X. Han, A. Jacobi, A review on polymer heat exchangers for HVAC&R applications, Int. J. Refrig. 32 (2009) 763–779, https://doi.org/10.1016/j.ijrefrig.2008.11.008.
[32] D. Pescod, An evaporative air cooler using a plate heat exchanger, CSIRO, Division of Mechanical Engineering., 1974.
[33] N. Klitsikas, M. Santamouris, A. Argiriou, D.N. Asimakopoulos, A.I. Dounis, Performance of an indirect evaporative cooler in Athens, Energy Build. 21 (1994) 55–63, https://doi.org/10.1016/0378-7788(94)90016-7.
[34] R.M. Lazzarin, A. Gasparella, New ideas for energy utilisation in combined heat and power with cooling: I. Principles, Appl. Therm. Eng. 17 (1997) 369–384, https://doi.org/10.1016/s1359-4311(96)00038-5.
[35] S. Delfani, J. Esmaeelian, H. Pasdarshahri, M. Karami, Energy saving potential of an indirect evaporative cooler as a pre-cooling unit for mechanical cooling systems in Iran, Energy Build. 42 (2010), https://doi.org/10.1016/j.enbuild.2010.07.009.
[36] G. Heidarinejad, M. Bozorgmehr, S. Delfani, J. Esmaeelian, Experimental investigation of two-stage indirect/direct evaporative cooling system in various climatic conditions, Build. Environ. 44 (2009), https://doi.org/10.1016/j.buildenv.2009.02.017.
[37] A. Bejan, G. Tsatsaronis, M. Moran, Thermal Design and Optimization, John Wiley & Sons, New York, 1996.
[38] P.E. Liley, Flow exergy of moist air, Exergy, An Int. J. 2 (2002) 55–57, https://doi.org/10.1016/S1164-0235(01)00039-5.

[39] C.Q. Ren, G.F. Tang, N.P. Li, G.F. Zhang, J. Yang, Analysis of Exergy of Moist Air and Energy Saving Potential in Hvac By Evaporative Cooling or Energy Recovery, 2 (2001) 113–117.

[40] W. W, C. JR, D. A, K. J, K. HJ, K. A, E. Al., The IAPWS industrial formulation 1997 for the thermodynamic properties of water and steam, J. Engine Gas, Turbines Power. 122 (2000) 150–170.

[41] A. Lazzaretto, G. Tsatsaronis, SPECO : A systematic and general methodology for calculating efficiencies and costs in thermal systems, Energy. 31 (2006) 1257–1289, https://doi.org/10.1016/j.energy.2005.03.011.

[42] A. Tejero-González, M. Andrés-Chicote, E. Velasco-Gómez, F. J. Rey-Martínez, Influence of constructive parameters on the performance of two indirect evaporative cooler prototypes, Appl. Therm. Eng. 51 (2013) 1017–1025, https://doi.org/10.1016/j.aquaculture.2010.10.030.

[43] A. Tejero-González, M. Andrés-Chicote, P. García-Ibáñez, E. Velasco-Gómez, F.J. Rey-Martínez, Assessing the applicability of passive cooling and heating techniques through climate factors: An overview, Renew. Sustain. Energy Rev. 65 (2016) 727–742, https://doi.org/10.1016/j.rser.2016.06.077.